VI

Publication VI

J. Oksanen and J. Tulkki, *Coherent optical logic by laser amplifiers with feedback*, accepted for publication in the IEEE Journal of Lightwave Technology **24** (2006).

Coherent optical logic by laser amplifiers with feedback

Jani Oksanen and Jukka Tulkki

***Abstract*— An optical decision circuit is constructed by modifying the stability conditions of a previously introduced optical flip-flop memory [1]. The simulations using a rate equation model of the circuit predict fast operation speed (rise and fall times of the order of 20 ps are reached) that is most likely beyond the capabilities of the recent semiconductor decision circuits suitable for integration [2]. The decision characteristics are also better, close to ideal digital response, and enable realizing optical logic gates by using an interferometer and a single decision circuit. The output characteristics of an AND and an OR -gate realized using the decision circuit are also studied.**

***Index Terms*— optical logic, decision circuit, optical transistor, coherent feedback**

I. Introduction

After the demonstration of the first ruby laser and various nonlinear optical effects in optical fibers in the 1960's, researchers started to develop the concept of an extremely fast digital optical computer [3]–[8]. In time, the original concept came in touch with the prevailing reality and evolved into a more earthly vision. At present some researchers believe that electronics and optics should be considered complementary technologies and that it is likely that optical solutions will not soon be used for the tasks traditionally achieved by electronics [9], [10]. Others pursue actively the rocky path leading to using optical logic in specialized small scale optical networking applications and possibly in transfering data inside electronic computers [11]–[14].

To be practical in even the simplest data processing applications, optical logic gates and other nonlinear devices should at least be fast and suitable for integration, have sufficient noise tolerance and stability and not to be overly power consuming. The optical logic gate prototypes known today fulfill many, but not all of these requirements.

The building blocks used for constructing optical logic devices have ranged from using long loops of optical fiber to the use of saturating semiconductor devices, such as optical amplifiers, lasers and bistable laser arrangements [2], [15]–[18]. The devices involving optical fibres are often fast (at least capable of operating at a few tens of GHz), but they are not suitable for integration. On the other end, the performance of the solutions based on semiconductor optical amplifiers or saturating laser amplifiers and interferometers is usually limited to a few GHz by the slow relaxation of carriers (nonradiative carrier lifetimes are of the order of 1 ns) or by the time it takes for a laser to recover from the saturated state.

This work introduces an optical decision circuit that is fast and provides a steep decision threshold that enables optical logic by interference. The device structure is based on an optical flip-flop circuit [1], [19] which is modified here in order to transform the bistable flip-flop circuit into a monostable decision circuit with a highly nonlinear input-output response. Although the circuit uses phase locked laser amplifiers, its operation does not involve saturating the lasers. Therefore its performance is not as severely limited by the carrier relaxation and saturation recovery processes as in the previously presented structures. If the challenges in processing the circuit are met, the device has potential as a versatile building block of simple optical data processing units. Section II gives a brief description of the device and completes the theoretical aspects to account for the asymmetry needed in making the device monostable. Section III shows the results of simulating the circuit and some examples on using it as an OR and an AND -gate. The actual rate equation model is given in the Appendix.

The authors are with the Department of Electrical and Communications Engineering, Helsinki University of Technology, Finland.

II. Theory and configurations

The operation of the logic gates presented in this work is based on the decision circuit making use of phase locked laser amplifiers with nonlinear feedback generated by interference of coherent waves. The theory laying ground for the operation has been presented recently in a study of an optical flip-flop circuit [19]. Here, the theory is extended to account for asymmetric feedback, which can disable the memory effect while retaining the highly nonlinear response characteristic of regenerative logical gates.

The schematic structure of the device with asymmetric feedback is shown in Fig. 1. The complete device composes of band stop filters, interferometric waveguide junctions, a possible additional amplifier in the feedback path and six laser amplifiers with three cavity modes each. The difference to the symmetric flip-flop structure is the wavelength selective transmission coefficients in the feedback path (t_{A1} and t_{A2} in Fig. 1) and the different transmission coefficients in the biasing waveguides (t_{B1} and t_{B2}). The wavelength selective transmission coefficients could be avoided if the injection currents to all laser amplifiers were not equal.

In brief, the power distribution of the modes in lasers L_1 and L_2 (and L_{A1} and L_{A2}) is determined by the feedback between the lasers and the input signal. Following [19] the steady state feedback equation for an idealized system with two phase locked lasers coupled to each other and injected with a constant bias signal can be written in the form

$$x = a_2\sqrt{1-\left(a_1\sqrt{1-x^2-s^2}+b_1\right)^2}+b_2 \qquad (1)$$

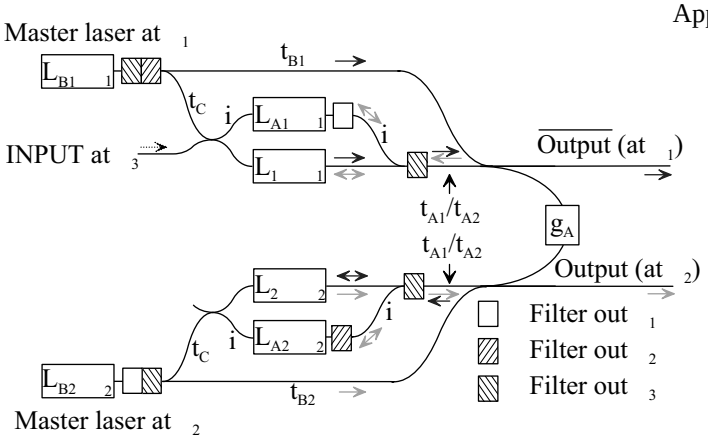

Fig. 1. The schematic device structure of the decision circuit. The decision circuit composes of six laser amplifiers, each supporting three cavity modes: λ_1, λ_2 and λ_3. The laser mode of each laser is either λ_1 or λ_2, as indicated by the number in the laser's name. The other modes have larger losses and are not lasing. Two of the lasers (L_{B1} and L_{B2}) only provide reference phase for the other lasers and bias signals for the feedback at wavelengths λ_1 and λ_2, respectively. Lasers L_{A1} and L_{A2} are identical to lasers L_1 and L_2 and they are used as a part of an antireflector structure to prevent unwanted feedback in the system. The transmission coefficients of the waveguides are indexed by symbols t_i, and the notation t_{A1}/t_{A2} means that the transmission of the waveguide is wavelength selective. The figure also includes an additional amplifier marked with g_A. Mode λ_3 is used to inject the input signal to lasers L_1 and L_{A1} and the output and inverted output are obtained from the corresponding output waveguides.

where x is the electric field at the input of laser L_1 (scaled so that $x_1 = 1$ when output is at its maximum), the coefficients a_i ($i \in \{1, 2\}$) describe the coupling strength between the lasers, b_i the strength of the bias field and s the input signal. Equation (1) may have up to four real solutions for a given value of s. At most two of these solutions describe the stable points of the idealized system (the other two are labile points). When more than one stable solution is found, the actual state of the decision circuit depends on the past values, and this leads to hysteresis in the circuit operation. The characteristic property of a stable state is that the laser mode power in one laser is decreased by the feedback, but the laser is not saturated. This situation is made possible by the bias signals. In Section III the stable solutions of Eq. (1) for selected configurations are calculated for comparison with the results obtained using the actual rate equation model.

The complete model of the circuit is based on coupled rate equations where the state of each laser is described by the carrier density and the complex electric field of each mode. For completeness, the rate equation model is given in the Appendix.

The coupling matrices $\mathbf{M}_U$, $\mathbf{M}_B$ and $\mathbf{M}_C$ in the rate equations describe the transmission coefficients of the wave guide network of Fig. 1 for the cavity modes λ_1, λ_2 and λ_3, respectively. They can be written as (see also [19] and the Appendix)

$$\mathbf{M}_U = \begin{bmatrix} 0 & C & iC & iB_1 & B_1 & 0 \\ C & 0 & 0 & iA_1 & A_1 & 0 \\ iC & 0 & 0 & 0 & 0 & 0 \\ iB_1 & iA_1 & 0 & 0 & 0 & 0 \\ B_1 & A_1 & 0 & 0 & 0 & 0 \\ 0 & 0 & 0 & 0 & 0 & 0 \end{bmatrix} \quad (2)$$

$$(\mathbf{M}_B)_{n,m} = \left[(\mathbf{M}_U)_{7-n,7-m}\right]_{|A_2 \to A_1,\, B_2 \to B_1} \quad (3)$$

$$\mathbf{M}_C = \mathbf{0} \quad (4)$$

$$A_i = \frac{1}{4}\sqrt{T_L T_s} g_A t_{Ai}^2 \quad (5)$$

$$B_i = A_i t_{Bi}/\sqrt{2} t_{Ai} \quad (6)$$

$$C = T_L t_C/2. \quad (7)$$

Here notation $|A_1 \to A_2$ is used for substituting A_2 for A_1 (and similarly B_2 for B_1) and T_L and T_s stand for the transmission coefficients of the laser facets for the optical power in the laser and signal modes, respectively. The symbols t_i refer to the electric field transmission coefficients of the waveguides of Fig. 1 and the additional gain g_A in the feedback path (also for electric field).

III. Results and discussion

The parameters used in the calculations are similar to those presented in [19], except for the asymmetric coupling parameters, shown in Table I. The parameter values are chosen to demonstrate the transition from a weakly nonlinear response without hysteresis (C1) to the strongly nonlinear response with hysteresis (C3). In addition to varying the coupling parameters, also the effect of changing the line width enhancement factor (LEF) and the additional gain g_A (and consequently the signal losses in the cavities) are studied.

Fig. 2 shows the operation characteristics of the three configurations of the decision circuit in steady state, as well as the output of the inverted output port and the solution of the idealized feedback equation in Eq. (1). In configuration C1 (Fig.2.a), the nonlinearity in the output is modest in comparison to the other two configurations, and the output exhibits no hysteresis. In configuration C2, the nonlinearity is stronger and the device is at the threshold where the output starts to exhibit hysteresis. The analytical approximation predicts stronger hysteresis than the results obtained from the more accurate model accounting for the gain compression and the light injected from the master lasers.

Configuration C3 exhibits clear hysteresis, although much less pronounced than the hysteresis of the symmetric structure used as an optical flip-flop [19]. The results of Fig. 2 are obtained by solving the initial value problem describing the system for a very slowly changing input signal under operating conditions where the input power is small enough not to saturate any of the lasers. If the lasers saturate, it takes a relatively long time to respond to changes in the input signal. Additionally, depending on the configuration, the output level may go below the desired logical high level even before saturation occurs. Therefore the input power should not exceed an upper limit where the operation properties deteriorate.

TABLE I

THE COUPLING PARAMETERS OF THE DIFFERENT DECISION CIRCUIT CONFIGURATIONS USED IN THE CALCULATIONS

Configuration	a_1	b_1	a_2	b_2	t_{A1}	t_{B1}	t_{A2}	t_{B2}
C1	1.5	-0.6	1.3	-0.6	1	-0.566	0.931	-0.566
C2	1.5	-0.6	1.7	-0.9	0.939	-0.499	1	-0.749
C3	2.1	-1.2	1.9	-1.2	1	-0.808	0.951	-0.808

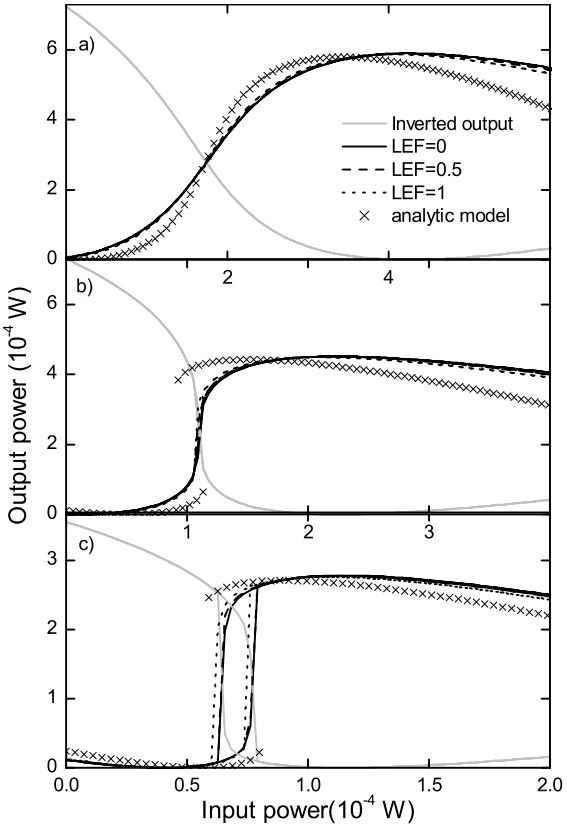

Fig. 2. The input-output relation of the decision circuit for different values of LEF and for the three configurations a) C1, b) C2 and c) C3. The curves labeled as 'inverted output' and 'analytic model' are the output of the inverted output port for LEF=0 and the stable solution of the idealized feedback equation given in Eq. (1).

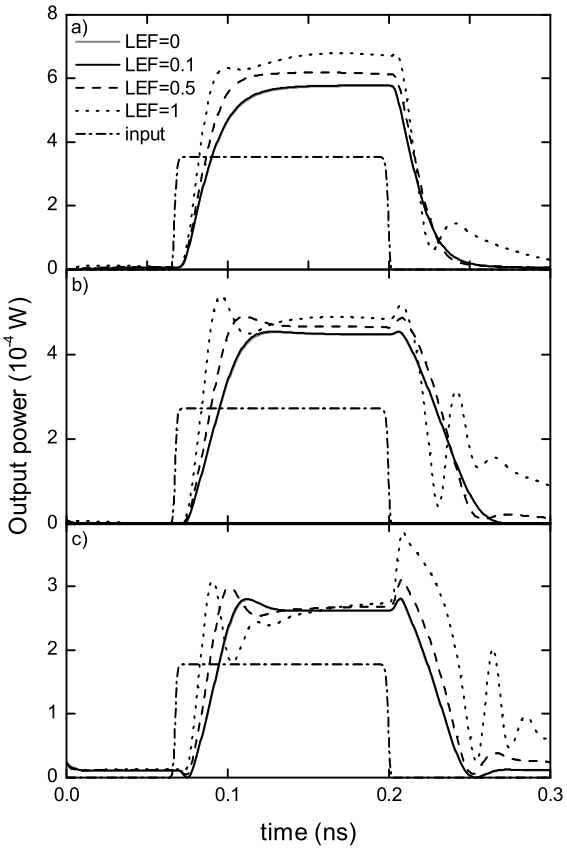

Fig. 3. The transient properties of the decision circuit for different values of LEF and configurations C1 (a), C2 (b) and C3 (c). Nonzero values of LEF introduce clear relaxation oscillations, whose origin is in the oscillation of the phase of the electric fields of the lasers. The additional amplification is $g_A = 4$ in these plots. The responses for LEF=0 and LEF=0.1 are almost identical and the corresponding curves overlap.

The maximum operating speed of the decision circuit depends on multiple factors. In Fig. 3 the transient response is calculated for the three configurations and for four values of LEF when a 0.13 ns pulse is applied to the input. The rise and fall times are of the order of 0.02 ns or more, and the oscillations caused by the phase relaxation for the larger values of LEF increase when moving from configuration one to configuration three. The 5 ps delay between the change in the input signal and any visible change in the output is mainly due to the propagation of the transient through the different modes of the lasers: first the change takes place in the signal mode of laser L_1, then in the laser mode of laser L_1 (at λ_1) followed by the feedback mode of laser L_2 (at λ_1), the laser mode of laser L_2 (at λ_2), and, finally the feedback mode of laser L_1 (at λ_2) and the output (at λ_2). In the inverted output the delay would be slightly shorter, since the inverted output is obtained directly from the laser mode of laser L_1. The output is shown only for a single input pulse to better demonstrate how the output power stabilizes towards its steady state value. The input pulses can be repeated when the output power is stabilized close to its steady state value. In the case LEF=0, this means that the repetition rate reaches approximately the value rise time + fall time.

The operating speed of the decision circuit mainly follows the response times of single laser amplifiers when LEF has a value close to zero. When LEF is not zero, the optical length of the lasers changes when the carrier densities in the lasers change and the phases of the lasers undergo a phase shift with respect to the phases of the master lasers. The properties of the feedback are altered and the output then features relaxation oscillations and slower operation. The dependence on the strength of the phase locking and the exact mechanism of the phase relaxation is out of scope of this study.

The single most important factor affecting the operating

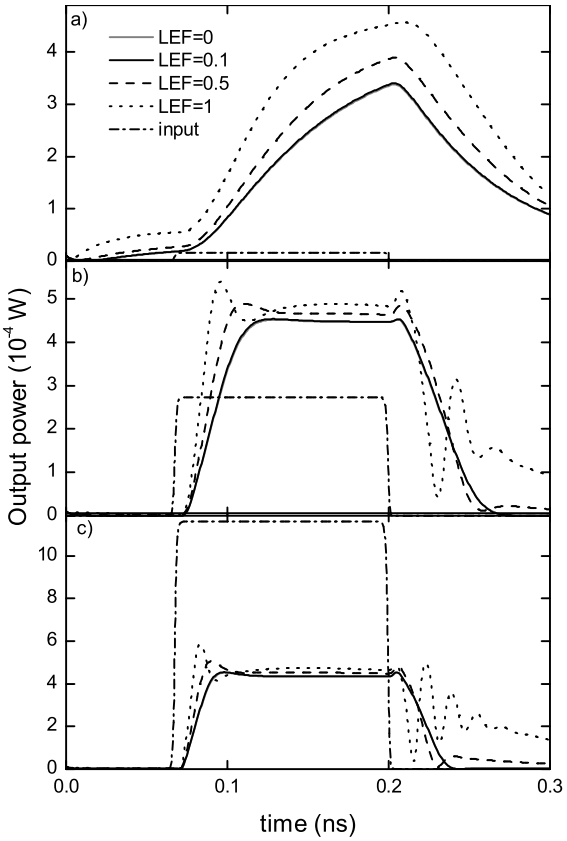

Fig. 4. The transient properties of configuration C2 for different values of additional gain g_A and LEF. a) There is no additional amplifier in the feedback path, ie $g_A = 1$, and the rise and fall times are large. b) The gain of the additional amplifier is set to $g_A = 4$ (the value used by default in the other calculations). The rise and fall times are relatively small. c) The gain of the additional amplifier is set to $g_A = 8$, which enables the fastest rise and fall times for the small values of LEF. The variations in the input signal power levels for different values of additional gain are due to changing the laser facet transmission coefficients and consequently the saturation injection power along with g_{A}. The responses for LEF=0 and LEF=0.1 are almost identical and the corresponding curves overlap.

speed of a single laser amplifier in the first order approximation is the total loss of the signal and feedback modes [20]. The largest possible magnitude of the total loss of the feedback mode, while still maintaining desired functionality in the circuit, is determined by the losses of the laser mode, the device geometry and the possible additional gain in the feedback path. The general tendency is that the losses of the signal mode can be increased if the losses of the laser mode or the additional gain increase or if the lasers become shorter. The physical limits for increasing the laser mode losses or shortening the cavity do not offer much liberty in enhancing the operation speed. Therefore the effect of the additional gain is interesting, since it can be easily adjusted. Fig. 4 shows the effect of adjusting the feedback gain and changing the cavity losses of the non-lasing modes of the lasers. The rise and fall times decrease from over 0.1 ns to 40 ps and to 20 ps, when the gain (for electric field) is adjusted from 1 to 4 and to 8, respectively.

Replacing basic logic gates with interferometers and optical 'transistors' or decision circuits has been a well known concept

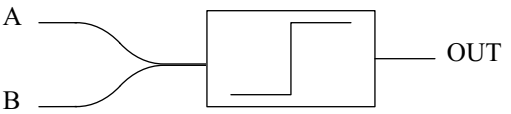

Fig. 5. A logic gate realized with an interferometer and a decision circuit. The phase shift θ controls the properties of the gate: with $\theta = 0$ the gate operates as an AND gate, and with $\theta = 110^\circ$ and OR gate.

in the past decades [8]. The basic idea is to make two signal interfere and then use the result as an input to a decision circuit (Fig. 5). An AND gate, for example makes two signals which alone do not pass the decision threshold, interfere constructively. When both the inputs are high, the signals interfere, the theshold is reached and the output goes high. The realization of such gates, however, has not had much success because of the lack of practical decision circuits.

To demonstrate the power of the decision circuit, some examples of using it to generate a logical AND and a logical OR gate are presented in Fig. 6. The gates are a trivial extension of the results shown in Figs. 2.b and 2.c with the input to the gate formed by two appropriately scaled signals. The interference is constructive ($\theta = 0$) for the AND gate and has a phase difference of $\theta = 110^\circ$ for the OR gate.

The steep decision characteristics of the decision circuits are also transferred to the logic gates, which have reasonably good correspondence to ideal logic gates. The worst property of the gates is that the individual inputs of the AND gates must not exceed a maximum value that could set the output high alone. Generally, any input values should also be small enough not to saturate the system.

The circular symmetry in the output is a characteristic property of this type of logic gates, using interferometers and coherent signals. Because of this symmetry, the noise margins of the gates can never quite match the noise margins of an ideal logic gate.

The model of the decision circuit is the same as used in the previous work with the optical flip-flops. Therefore the inaccuracies of the model, mainly the exclusion of the noise and the propagation delay between the lasers, also remain the same. However, since systems with feedback are generally very tolerant to noise and the power of the amplified spontaneous emission is generally small compared to the power emitted by the lasers, the noise generated by spontaneous emission is not expected to be a problem. Although the effect of the two inaccuracies should be small and the model itself can be considered reasonably accurate, their effects, the tolerances for unideal device parameters and the effects of phase locking in general should be studied in more detail. This, however, is out of scope of this manuscript.

The speed of the decision circuit is fundamentally limited by the GCSOA. The limiting frequency is approximated by $v\left(\alpha_s - G_s\right)/20$ (or $v\alpha_L$, if it is smaller) [20], where α_s and α_L are the cavity losses of the signal mode and the laser mode, respectively and G_s is the gain of the signal mode. The term $\alpha_s - G_s$ is mainly limited by technology, and with increasing ability to process optical devices the operating speed may be expected to rise well beyond 100 GHz.

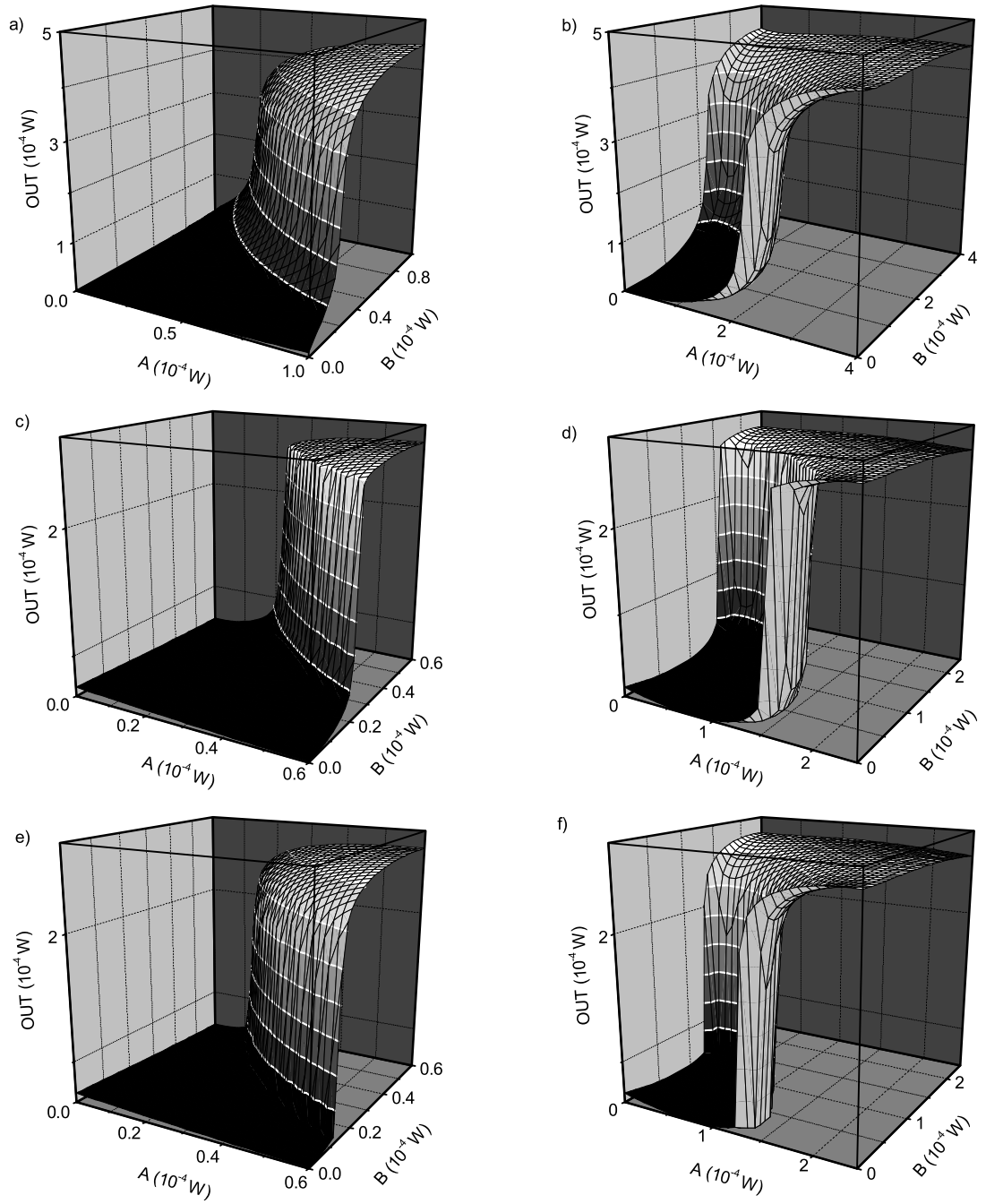

Fig. 6. The response of the AND gates (left) and the OR gates (right) realized with an interferometer and the decision circuit (Fig. 5). Inputs A and B are two coherent inputs to the interferometer and OUT is the output from the decision circuit. The gates a) and b) are realized using configuration C2. The other gates are calculated for the two hysteresis loops of configuration C3. Configuration C1 is not sufficiently nonlinear to be used as a logic gate.

The input signals to the logic gate structure presented in this paper need to be coherent, their phase difference needs to be controlled and their power level must be within certain limits. If the signals are originally not coherent or they have random phase, additional phase locked GCSOAs or other devices to lock the phases are needed. In a traditional optical network with isolated logic gates distributed across the network this would be highly unpractical. However, if the logic gates, memories and other coherent nonlinear circuits are placed very close to each other, say on an integrated circuit performing some simple task, the situation changes drastically. In the small scale of an integrated circuit the phase differences and powers of the signals are no longer subject to (strong) random fluctuations but determined mostly by the geometry and properties of the circuit. Then the coherence and well determined phase are no longer stringent requirements, but just properties of the signal.

Variations of all the individual components used in the construction of the decision circuit have already been demonstrated separately. The gain clamped semiconductor amplifiers, interferometers and band stop filters as such are practically standard components. The phase locking and gain spectrum of the GCSOAs in this work are, however, somewhat peculiar. The band stop filters of the device only need to process the three wavelengths λ_1, λ_2 and λ_3 and they should be realizable for example using filters based on of Mach-Zehnder interferometers [21], [22], coupled waveguides or in the future photonic crystals. The main concern in the realization of the decision circuit is the accurate phase control and processing of the individual components on the same chip with sufficient quality. If the optical technologies continue to evolve coherent optics may find many uses in applications that can not be practically realized today.

IV. Conclusions

This work introduces asymmetric feedback in a previously introduced optical flip-flop memory model in order to remove the memory effect but still enable very nonlinear decision circuit -type output. The simulations of the circuit predict faster operation (rise and fall times of the order 20 ps) and steeper decision threshold than in the previously introduced active semiconductor devices suitable for integration. The fast operation is based on a new feedback configuration which allows the laser amplifiers of the structure to operate above their saturation limit. Also logical AND and OR gates based on the structure are demonstrated.

The decision circuit composes of six laser amplifiers connected by a network of wave guides and filters. Despite the apparent complexity, the structure is in principle suitable for integration. Some of the material parameters required for good performance are at the limit of feasibility (most notably the maximum modal gain, transparency carrier density and the linewidth enhancement factor of the lasers), but processing functional prototypes should be possible with less stringent requirements.

The stucture has potential as a versatile building block for integrated optical circuits. The same structure with minor modifications enables fast optical logic, optical memory and synchronous optical data processing in integrated small scale optical devices, all at once.

Appendix

In vector form the rate equations used in this work to describe the system of Fig. 1 can be written as

$$\frac{d\mathbf{n}}{dt} = \frac{I}{qV} - \sum_{j\in\{U,B,C\}} 2\xi v \mathbf{G}_j(\mathbf{n}) |\mathbf{E}_j|^2 - \frac{\mathbf{n}}{\tau} \quad (8)$$

$$\frac{d\mathbf{E}_j}{dt} = \frac{v}{2}\left[\mathbf{G}_j(\mathbf{n}) - \boldsymbol{\alpha}_j + i\Delta\boldsymbol{\omega}_j(\mathbf{n})\right]\mathbf{E}_j + \frac{v}{2L}\mathbf{E}_j^{\text{ext}} + \frac{v}{2L}\mathbf{M}_j\mathbf{E}_j. \quad (9)$$

Each component of the carrier density $\mathbf{n}$ and of the propagating complex electric field $\mathbf{E}_j$ of the cavity mode $j \in \{U, B, C\}$ (U stands for the mode λ_1, B for λ_2 and C for λ_3) is associated with one laser amplifier. I, q and V are the injection current, elementary charge and cavity volume, respectively. The term $\xi = \sqrt{\varepsilon\mu^{-1}}/(2\hbar\omega v)$ is the conversion factor that transforms the square of the absolute value of the electric field to photon density. The factor 2 in front of ξ in Eq. (8) results from the presense of the two counter propagating electric fields. The diagonal matrix $\mathbf{G}_j(\mathbf{n})$ contains the modal gains of each laser for mode j. The absolute value in Eq. (8) is applied to each component of $\mathbf{E}_j$ independently. Interband transitions that are not caused by stimulated emission (mainly nonradiative interband transitions and spontaneous emission) are described by the vector $\mathbf{n}/\tau$, where τ is the average lifetime of the carriers close to the lasing threshold.

The diagonal matrices $\boldsymbol{\alpha}_j$ contain the cavity losses for the mode j in each laser and the diagonal matrices $\Delta\boldsymbol{\omega}_j(\mathbf{n})$ contain the displacements of the frequency of the mode j from the corresponding cavity resonance. The length of the cavity is denoted by L and $\mathbf{E}_j^{\text{ext}}$ is a vector describing the fields injected from outside the cavity. The coupling matrices $\mathbf{M}_j$ are off-diagonal and describe the coupling between the lasers.

For a more complete description of the model and used parameters, see [19].

References

[1] J. Oksanen and J. Tulkki, "A fast coherent all-optical flip-flop memory," *Appl. Phys. Lett.*, 2005. waiting to be accepted.

[2] W. D'Oosterlinck, G. Morthier, M. K. Smit, and R. Baets, "Very steep optical thresholding characteristic using a DFB laser diode and an SOA in an optical feedback scheme," *J. Lightwave Technol.*, vol. 17, pp. 642–644, Mar. 2005.

[3] T. H. Maiman, "Stimulated optical radiation in ruby," *Nature*, vol. 187, pp. 493–494, Aug. 1960.

[4] P. A. Franken, A. E. Hill, C. W. Peters, and G. Weinreich, "Generation of optical harmonics," *Phys. Rev. Lett.*, vol. 7, pp. 118–119, Aug. 1961.

[5] R. Y. Chiao, C. H. Townes, and B. P. Stoicheff, "Stimulated Brillouin scattering and coherent generation of intense hypersonic waves," *Phys. Rev. Lett.*, vol. 12, pp. 592–595, May 1964.

[6] A. Szöke, J. Daneu, J. Goldhar, and N. A. Kurnit, "Bistable optical element and its applications," *Appl. Phys. Lett.*, vol. 15, pp. 376–379, Dec. 1969.

[7] A. A. Shawchuk and T. C. Strand, "Digital optical computing," *Proc. IEEE*, vol. 72, pp. 758–779, July 1984.

[8] M. N. Sriharshavardhan, "Optical computers," *IEEE Potentials*, vol. 15, pp. 17–20, Apr. 1996.

[9] A. Jajszczyk, "Optical networks - the electro-optic reality," *Optical switching and networking*, vol. 1, pp. 3–18, Jan. 2005.
[10] H. J. Caulfield, "Perspectives in optical computing," *IEEE Computer*, vol. 31, pp. 22–25, Feb. 1998.
[11] F. Ramos, E. Kehayas, J. M. Martinez, R. Clavero, J. Marti, L. Stampoulidis, D. Tsiokos, H. Avramopoulos, J. Zhang, P. V. Holm-Nielsen, N. Chi, P. Jeppesen, N. Yan, I. T. Monroy, A. M. J. Koonen, M. T. Hill, Y. Liu, H. J. S. Dorren, R. V. Caenegem, D. Colle, M. Pickavet, and B. Riposati, "IST-LASAGNE: towards all-optical label swapping employing optical logic gates and optical flip-flops," *J. Lightwave Technol.*, vol. 23, pp. 2993–3011, Oct. 2005.
[12] M. Forbes, J. Gourlay, and M. Desmulliez, "Optically interconnected electronic chips: a tutorial and review of the technology," *Elect. & Comm. Eng. J.*, vol. 13, pp. 221–232, Oct. 2001.
[13] D. J. Blumenthal, J. E. Bowers, L. Rau, H.-F. Chou, S. Rangarajan, W. Wang, and H. N. Poulsen, "Optical signal processing for optical packet switching networks," *IEEE Commun. Mag.*, vol. 41, pp. S23–S29, Feb. 2003.
[14] M. Soljačić and J. D. Joannopoulos, "Enhancement of nonlinear effects using photonic crystals," *Nature Materials*, vol. 3, pp. 211–219, Apr. 2004.
[15] A. Bogoni, L. Potí, R. Proietti, G. Meloni, F. Ponzini, and P. Ghelfi, "Regenerative and reconfigurable all-optical logic gates for ultra-fast applications," *Electr. lett.*, vol. 41, pp. 435–436, Mar. 2005.
[16] M. T. Hill, H. de Waardt, G. D. Khoe, and H. J. Dorren, "All-optical flip-flop based on coupled laser diodes," *IEEE J. Quantum Electron.*, vol. 37, pp. 405–413, Mar. 2001.
[17] G. Morthier, M. Zhao, B. Vanderhaegen, and R. Baets, "Experimental demonstration of an all-optical 2R regenerator with adjustable decision threshold and 'true' regeneration characteristics," *IEEE Photon. Technol. Lett.*, vol. 12, pp. 1516–1518, Nov. 2000.
[18] M. T. Hill, H. J. S. Dorren, T. de Vries, X. J. M. Leijtens, J. H. den Besten, B. Smalbrugge, Y.-S. Oei, H. Binsma, G.-D. Khoe, and M. K. Smit, "A fast low-power optical memory based on coupled micro-ring lasers," *Nature*, vol. 432, pp. 206–209, Nov. 2004.
[19] J. Oksanen and J. Tulkki, "Fast all-optical flip-flop memory exploiting the electric field nonlinearity of coherent laser amplifiers," *IEEE J. Quantum Electron.*, 2006. waiting for sending.
[20] J. Oksanen and J. Tulkki, "Fast 2R regeneration by coherent laser amplifiers," *IEEE J. Quantum Electron.*, vol. 41, pp. 1075–1082, Aug. 2005.
[21] T. Segawa, S. Matsuo, Y. Ohiso, T. Ishii, Y. Shibata, and H. Suzuki, "Fast tunable optical filter using cascaded Mach-Zehnder interferometers with apodized sampled gratings," *IEEE Photon. Technol. Lett.*, vol. 17, pp. 139–141, Jan. 2005.
[22] R. Ramaswami and K. N. Sivarajan, *Optical networks, A practical perspective*. Morgan Kaufmann Publishers, Inc, 1998.